

A Prioritized Satellite Task Scheduling Model Based on the Fewer Observation Opportunities

Mohamed Atef Mosa,

Information Technology Sector, Institute of Public Administration, Riyadh, KSA.

Egyptian Space Agency, Assembly, Integration & Testing Center, Cairo, Egypt.

mosamo@ipa.edu.sa, mohammedatefmosa@gmail.com

Abstract: The turbulent nature of catalytic reactions has been well reported. For some reactions, the higher the rate of turbulence, the faster the reaction process. This paper focus on the review of various research works where turbulence models were employed in promoting and advancing study and knowledge of catalysis or catalytic reaction systems (such as fixed bed reactor, trickle bed reactor, combustor, among others) or processes in the twentieth centuries. It also draws attention to several fluid computational dynamics package employed in the simulation and different contributions that have been made in advancing research in the field of catalysis via turbulence modeling. The essence of these is to enhance effective and efficient reactant access to the active sites of the catalyst. This study, however, shows that models such as k-e and RSM turbulence models are better suited for predicting or studying turbulence behavior in a catalytic reaction. It was realized that apart from selecting the turbulence model, appropriate selection of the kinetic model plays a significant role in promoting accurate prediction when carrying out simulations. However, this study was able to identify that only a few research works have given attention to the right and appropriate use or selection of a kinetic model for catalytic reaction systems.

Keywords: Simulation, Transport Phenomena, Kinetic Model, Chemical Reactors, Turbulence.

نموذج جدولة مهام القمر الصناعي ذو الأولوية استناداً إلى فرص المراقبة الأقل

الملخص: تلعب موارد الأقمار الصناعية لرصد الأرض دوراً رائداً في تعزيز أنظمة المراقبة متعددة الأقمار الصناعية. في هذا البحث، تم اقتراح نهج جديد يعتمد على خوارزمية تحسين مستعمرة النمل (ACO) بالاندماج مع خوارزمية تصنيف الصفحات PageRank لتعظيم فترة التصوير لجميع الأهداف المطلوبة تحت شروط معينة. تم تكوين دالة الملاءمة بناءً على العديد من الميزات المحورية لتحقيق الأداء الأمثل ورضا العملاء. تمت إعادة صياغة نموذج PageRank لتصنيف الأهداف بناءً على الأولوية استجابةً لفرص المراقبة الأقل، بحيث لا يتم فقدانها إلى الأبد. أخيراً، أثر متغيرات المنهج المدروسة بالطرق التجريبية. تم تحليل أداء النهج ومقارنته بالدراسات الموجودة. تظهر النتيجة التجريبية أن نهج SEOSR يؤدي أداءً أفضل من الخوارزميات الحالية، وأن خوارزمية PageRank قادرة على تحسين عملية الجدولة الإجمالية والحفاظ على بعض المهام من الضياع. وأخيراً، حققت الخوارزمية المقترحة كفاءة تزيد عن ٩٠٪ مقارنة بالطرق الأخرى.

1. Introduction:

The Schedule Earth Observation Satellite Resources (SEOSR) task is a type of combinatorial optimization problem regarding the aerospace field. It is one of the prime tasks of satellite missions, such as ground-based satellite tracking and telemetry/command network. SEOSR specializes in how to nominate time windows and resources to multi-mission properly during a certain time. A lot of work has been done to tackle the multi-satellite scheduling problem. Several conventional optimization models are not suitable for SEOSR. Moreover, many types of research have been developed using heuristic methods to solve this task. (Frank, J. et al. 2001) modeled the problem to be associated with its constraints that are used based on the interval planning framework and heuristic search technique. Unfortunately, the authors have not considered the task conflict case in an experimental result. Moreover, many researchers have employed a tabu search (TS) algorithm to tackle the scheduling issue (Sarkheyli, A. et al. 2010) (Zufferey, N. et al. 2008) (Bianchessi, N. et al. 2007). The TS algorithm has been used to test satellites associated management with their orbits to carry out a lot of satisfied requests under several complicated conditions (Bianchessi, N. et al. 2007). Moreover, the TS heuristic is also developed for the multi-resource scheduling problem by adopting a memory capacity that contains all the feasible schedules. These heuristics are created from an effective theory of graph coloring. Numerical experiments showed a robust algorithm outperforms other mechanisms depend on the alteration solution space (Zufferey, N. et al 2008). The authors (Sarkheyli, A. et al. 2010) developed the near-optimal and feasible schedule for earth observation. They have introduced the TS heuristic method based on the time constraint for solving the scheduling task. On the other hand, (Marinelli, F. et al. 2011) proposed a Lagrangian heuristic for the scheduling problem. The Lagrangian has consisted of a sequence of maximum independent weighted that shown on interval graphs.

With the enhancement of brilliant optimization methods, several types of research intelligently turn to use optimization techniques for solving the scheduling task. Genetic algorithm (GA) is one of the algorithms that has been employed to strengthen the scheduling task (Barbulescu, L. et al. 2002). The worst present solutions created are replaced by the best ones. For a broad range of problem instances, the authors in (Barbulescu, L. et al. 2002) observed that a genetic algorithm named 'Genitor' done well. A new GA and an appropriate GUI construction for an autonomous satellite to simulate a scheduling task is developed (Baek, S. et al. 2011). The idea in (Zhu, K. et al. 2010) considered the satellite scheduling and orbit design problems for

realizing optimal disaster rescue. On the other hand, several types of research have formulated the scheduling task for solving as a multi-objective optimization MOO problem. It was undertaken by the hybrid algorithm of particle swarm optimization (PSO), which is a new idea for orbit design. The authors in (Chen, Y. et al. 2012) proposed a new GA-PSO by combining the PSO and genetic algorithm for building an optimization model based on deep analyses of the scheduling characteristics.

Ant colony optimization (ACO) is a skillful algorithm in solving all kinds of optimization problems (Mosa, M. A. et al. 2017a, Mosa, M. A. et al. 2017b, Mosa, M. A. et al. 2017c, Thiruvady, D. et al. 2019, Mosa, M. A. et al. 2020, Mosa, M. A. et al. 2017c). A novel optimization algorithm is proposed in (Zhang, N. et al. 2011) using guidance-solution (GsB-ACO) to solve the scheduling task. They advanced a set of guidance solutions for avoiding premature convergence. Additionally, to reach a promising space relative rapidly. Once the algorithm stagnation, update pheromone has been developed by changing its distribution based on the guidance of the solutions. The authors (Gao, K. et al. 2013) Adapted the ACO algorithm by combination with an iteration local search method (ACO-ILS) to resolve the multi-satellite observation scheduling task. They constructed an acyclic directed graph for the searching process. Later, the ILS method is utilized for further solution enhancement initially obtained by ACO. The authors (Gao, K. et al. 2013) proposed a scheduling system by clustering more than one task with mutual features. It is noteworthy that Gravitational Search Algorithm GSA has been employed in several real-time applications (Mosa, M. A. et al. 2019a), but so far this algorithm has not been used to solve the satellite scheduling task.

In this study, a novel approach in addressing the multi-satellite missions scheduling for earth observation is proposed. This approach aims to enhance scheduling effectiveness from a new point of view. Firstly, several customers may demand several targets (polygon area) to be observed at a certain time. Some characteristics of images have to be addressed before the observation. One of those characteristics is the resolution of the image. The resolution mostly depends on the degree of slewing angle (i.e., when the satellite turns right or left to observe the target). The second demand that must be predefined is the acceptable ratio of the coverage area of the target. In this case, it is not compulsory to observe the entire target. The principal objective of this approach is to schedule the missions of satellite constellations to observe many targets and to communicate with the ground data reception station (GDRS) for sending data and receiving telecommand parameters. We formulated the earth observation task to an

optimization problem in a novel shape by maximizing the profit of observation for all demanded targets that are satisfying certain conditions. To accomplish this issue, the ACO is employed to obtain the optimal schedule for the earth observation task. ACO is a master algorithm in solving optimization tasks (Mosa, M. A. et al. 2019b) showed that the ACO's convergence is proven analytically, whereas most other meta-heuristic models anticipating convergence are just depending on experimentation. The crucial factor in the scheduling issue is the customers only accept the target if the acceptable ratio of the target is satisfied. Otherwise, the target would reject. Moreover, many of those targets mostly lost forever in case of a lack of observation of their strips early. The main contribution of this paper is centered around how to observe targets based on the priority in response to fewer observation opportunities for strip ranking. Therefore, a PageRank algorithm mixed with ACO in a new form to be to fulfill this issue. The main idea behind the rank of strips is to know which targets have fewer observation opportunities to be scheduled first in the plan. The PageRank algorithm is employed to come down the target loss as possible and enhance the effectiveness of the scheduling task.

The remainder of the paper is structured as follows. Section 2 presents the problem definition containing a general description and mathematical model. In section 3, the proposed approach of earth observation is illustrated. Section 4 exhibits other approaches developed for comparison and evaluation. Section 5 provides conclusions.

2. Problem definition

In this section, we present a general description and mathematical model of SEOSR.

2.1. General description

The satellites in their orbits shall connect to the ground stations several times a day. Those ground stations receive telemetry data about the satellite to monitor the state of its health and send telecommand via the antennas to keep working efficaciously. Additionally, the satellites transmit information (i.e., images) to those ground stations. Generally, one satellite may need to communicate four to six times all day long by one or more antennas according to its state. Each ground station has two antennas, i.e., S/X-bands. It even may be visible to many antennas simultaneously. When more than one satellite passes over the same antenna meanwhile, there is a conflict between them because an antenna can solely serve one satellite at a time. There are three stages (i.e., modes) to the satellite ready to observe the earth. The first mode is a "preparation mode" to power on the types of equipment that responsible for turning the satellite.

The second one is an "orientation mode" to enable the satellite of turning to reach a demanded angle. The third one is a "stabilization mode" that is responsible for open the cameras for observation. On the other hand, different customers may order various types of targets for emergency observation with a certain percentage of the coverage acceptance area in a certain time. If the coverage area of demanded targets does not reach the acceptable percentage, these targets are neglected. The target is mostly classified into two types, emergency, and normal target. The priority of the emergency target is more than the normal one. The single target may be divided into many strips. When there is no except one opportunity to observe the emergency or normal task, the approach selects the emergency one to be scheduled. With an increasing number of satellites, it is turning into more challenging to produce effective schedules manually. Therefore, the SEOSR can be represented to maximize the profit observation of targets by assigning the time windows for satellites, and the resolution of targets under certain constraints. Depending on the above depiction, the SEOSR can be described by four-tuple: {targets, resources, constraints, and optimize objects}, where targets are areas that in needing of observation by the satellite. The resources commonly indicate the monitoring/control equipment.

2.2. Mathematical problem representation:

In the problem of multi-satellite resource scheduling, there are several satellites, ground stations, and many polygon targets in need of being assigned to a certain satellite in a particular orbit. The purpose of the satellite observation schedule is to organize a series of observations for each satellites' orbit to maximize the profit of observation with high resolution, subject to certain complex constraints. For simplicity, many various satellites' orbits can be considered as the same type of observation capabilities and resources. Let $O = \{o_j, j = 1, 2, \dots, M\}$ is the list of orbits, where M represents the total number of satellites' orbits. $T = \{t_i, i = 1, 2, \dots, N\}$ denotes list of targets t_i , where N represents the total number of targets. The target t_i comprised of one or more strip $S = \{s_{ki}, k = 1, 2, \dots, L\}$, where L represents the total number of strips belong to target t_i . Decision variable x_{kij} indicates eventually whether strip s_k that belongs to target t_i is scheduled to be accomplished on-orbit o_j .

$$x_{kij} = \begin{cases} 1 & \text{if strip } s_k \text{ of target } t_i \text{ is sceduled to be excuted in orbit } o_j \\ 0 & \text{otherwise} \end{cases} \quad (1)$$

If orbit o_j has no visibility for strip s_{ki} , x_{kij} is set to zero. Some relevant notations and parameters used in the model are defined as shown below.

$TW_{ki} = [ts_{ki}, te_{ki}]$	The possible time-window of a strip s_k for target t_i in an orbit o_j .
$TWd_{ki} = [tsd_{ki}, ted_{ki}]$	The possible time-window of downlink a strip s_k for target t_i in an orbit o_j .
p_{ki}	Priority associated with a strip s_k for target t_i
ty_{ki}	Type of a strip s_k for target t_i .
y_{kihl}	1–0 variable pointing out whether a strip s_{hl} will be executed after s_{ki} .
W_j	Memory storage capacity in an orbit o_j .
w_j	Memory consumption rate in an orbit o_j
E_j	Energy capacity in an orbit o_j .
eo_j	Energy consumption rate by observation in an orbit o_j .
es_j	Energy consumption rate by a sensor slewing observation in an orbit o_j .
ed_j	Energy consumption rate by downlinking in an orbit o_j .
v_j	Sensor slewing velocity in an orbit o_j .
a_j	Setup time required for opening and calibrating the sensor in an orbit o_j .
θ_{ki}	Slewing angle to observe a strip s_k for target t_i in an orbit o_j .
ns_k	Number of strips s_k in target t_i
c_j	Maximum times for a satellite opening its sensor in an orbit o_j .
ap_i	Percentage of acceptance a target t_i
ov_i	Percentage of overlapping in target t_i
po_{mi}	Point po_m for a target t_i

The objective function is maximizing the total profit of the resources by selecting the long strips which have high priorities.

$$\max \sum_{j=1}^M \sum_{i=1}^N x_{kij} * p_{ki} * TW_{ki} \quad k = 1, 2, \dots, L \quad (2)$$

On the other hand, the complex constraints which have to be taken into consideration are described below (Gao, K. et al. 2013).

$$\sum_{j=1}^M x_{kij} \leq 1, \quad i = 1, 2, \dots, N, \quad k = 1, 2, \dots, L \quad (3)$$

$$ts_{ki}, te_{ki} \geq a_j + (|\theta_{ki}| + |\theta_{ha}|) / v_j, \quad i, a = 1, 2, \dots, N, j = 1, 2, \dots, M, k = 1, 2, \dots, L \quad (4)$$

$$\sum_{i=1}^N x_{kij} * eo_j * (te_{ki} - ts_{ki}) + \sum_{i=1}^N \sum_{h=1}^N x_{kij} * x_{hlj} * y_{kihl} * es_j \left(\frac{a_j + (|\theta_{ki}| + |\theta_{ha}|)}{v_j} \right) \leq E_j, \quad j = 1, 2, \dots, M \quad k, h = 1, 2, \dots, L \quad (5)$$

$$\sum_{i=1}^N x_{kij} * w_j * (te_{ki} - ts_{ki}) \leq W_j, j = 1,2, \dots, M, k = 1, 2, \dots, L \quad (6)$$

$$\sum_{i=1}^N x_{kij} \leq c_j, j = 1,2, \dots, M, k = 1, 2, \dots, L \quad (7)$$

$$\sum_{j=1}^N ns_k \geq ap_i, i = 1, 2, \dots, N, k = 1, 2, \dots, L \quad (8)$$

Constraint (3) demonstrates that each strip requires to be just observed one time by one satellite within any orbit. Constraint 4 shows a sufficient setup time needed for a satellite to work its sensor (in the preparation stage) and orient to reach a predefined angle (in the orientation phase). Constraint (5) means that every satellite is not permitted to consume energy more than the limit permissible in orbit. The energy is considerably consumed by the sensors that are responsible for slewing and observation. Constraint (6) means that every satellite is not permitted to exceed the size of memory capacity in orbit. Constraint 7 means that any satellite needs a sufficient amount of time to run its sensor before executing an observation task (i.e., during the stabilization or imaging mode). Additionally, at each orbit, the time to operate a camera is restricted to a predefined time. Constraint (8) means that the size of strips observed of a certain target must be equal to or more than the demanded acceptance percentage that had predefined by the customer. In other words, it is not admissible to observe further strips of a certain target when the demanded percentage of the target is satisfied.

3. Proposed framework for ACO-SRSEO:

In this section, the detail of the SEOSR approach is expressively demonstrated. The overall process of the approach unravels to illustrate its parts as plotted in Figure. 1.

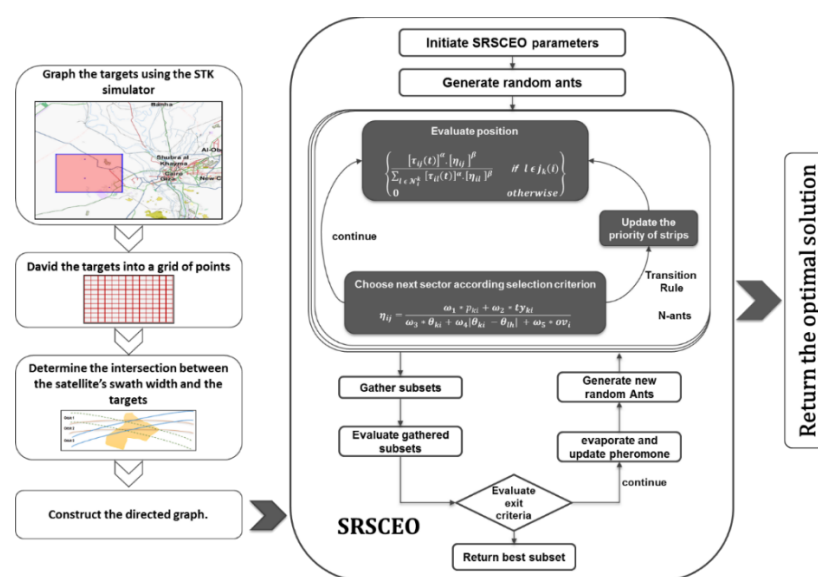


Figure No. 1: System model of the proposed approach.

Firstly, all proposed targets plot on the map using the Satellite Tool Kit (STK) simulator, ballistic information for future orbits is obtained according to a preparation phase in section 3.1. Later, a sly algorithm divides these targets (polygon area) into a grid of latitude and longitude points as shown in section 3.2. Subsequently, to divide each polygon target into a set of strips, different strips are obtained relied on the intersection between the satellite's swath width and all targets as presented in section 3.3. The strip length depends on the period of observation time and must satisfy constraint NO. 7. The width of a strip depends on the inner and outer half-angle, as illustrated in Figure. 2. For simplicity, we assume the widths of all strips are equal. Moreover, the interference between different orbits and strips will inevitably be because multiple strips may be generated in the same satellite projection by changing the satellite's slewing angles. Several strips are generated for the algorithm to decide which strip is more desirable. Later, the priority for every strip is obtained using the PageRank algorithm depending on the number of observations as shown in section 3.4. Finally, to maximize the profit of observation with high resolution, we employed the ACO to obtain the best schedule as elaborated in section 3.5. Additionally, the PageRank algorithm is mixed with ACO for performance enhancement of the approach in terms of the number of targets observed. During the iterations, when no further optimization arises in the fitness function for several sequential iterations and no constraints are breached, the program stops. In this section, the detail of SEOSRis demonstrated in the pseudo-code below.

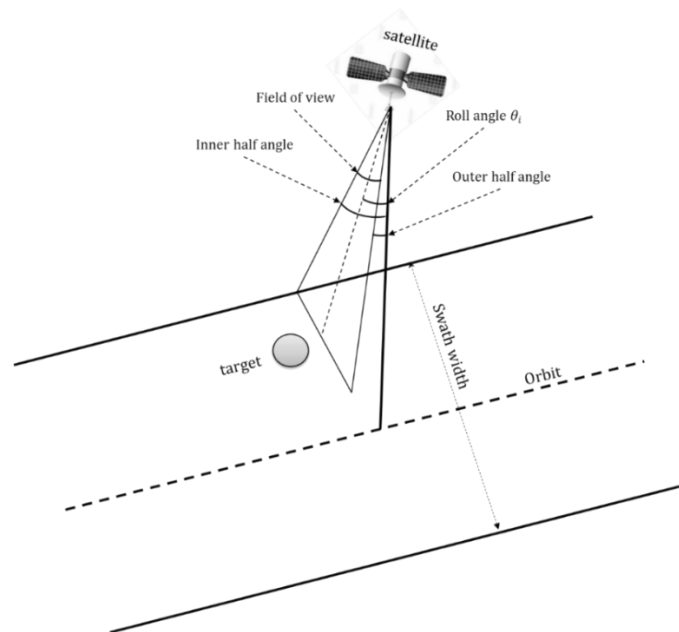


Figure No. 2: Observation process of the satellite

3.1. Preparation data.

Firstly, the operation centre of all ground stations receives various targets that in need of observation from many customers simultaneously. The data of imaging shall be determined by customers such as 1) the needed ratio of coverage area, 2) the resolution of the target has to come down a threshold, 3) time of delivery, 4) type of cameras and channels, 5) and finally, type of imaging (i.e., emergency). Later, all targets plot on the map using the STK simulator, and the ballistic information and the navigation parameters in terms of the future orbits are obtained for positioning satellites in the future.

3.2. Dividing the target into a grid of points

Second, we partitioned the polygon targets into a grid of small squares expressed by the longitude and latitude of their angles. The main objective of segmenting the polygon targets is to verify and follow up on the required observable percentage of the target.

3.3. Determine the intersections between the satellite's swath width and targets.

Satellite swath width is the boundary of the projected area on the earth, where the satellite can maneuver and reach the maximum slewing angle within it. The big targets can't be observed in one shot. Therefore, many polygon targets need to divide into many strips. Each strip contains a set of points that are observed by the same slewing angle. Since the strip constraints are related to the sensor slewing angle and a time window. So, these parameters shall be calculated. The time window is denoted by Δt . Multiple points can be clustered together to be observed by a sensor with the same slewing angle and swath width. Therefore, a rational procedure of splitting big targets is also developed taking into consideration maximum slewing angle, time window, and overlapping among multiple strips.

3.4. Graph Representation

According to the altitude of a satellite, it may classify satellites into three types. 1) A high earth-orbit (HEO) satellites, 2) a middle-earth-orbit (MEO) satellites 3) a low-earth-orbit (LEO) satellite. In this paper, we focus on the LEO satellites. One cause is that the time windows for an LEO satellite are usually much shorter than other types. Secondly, the limitation of LEO satellite resources causes a narrow coverage of satellite orbits. All strips generated are linked with each other when satisfying all mentioned constraints based on the

precedence and the satellite direction. Based on possible observation orders of strips, an acyclic directed graph model is constructed for each orbit. As shown in Figure. 3, generated strips denote the nodes that satisfy setup time constraint NO. 4 will be linked by a directed edge (i.e., indicate that one task can be executed successively after another). The edges are the relationship among the nodes based on the precedence. Note that the same strip may belong to more than one different orbit. For instance, in Figure. 3, tasks S8 and S10 have time windows in both orbit#1, orbit#2, and orbit#3 simultaneously. The latter scheduling algorithm determines strips S8 and S10 to be executed whether in orbit#1, orbit#2, or orbit#3.

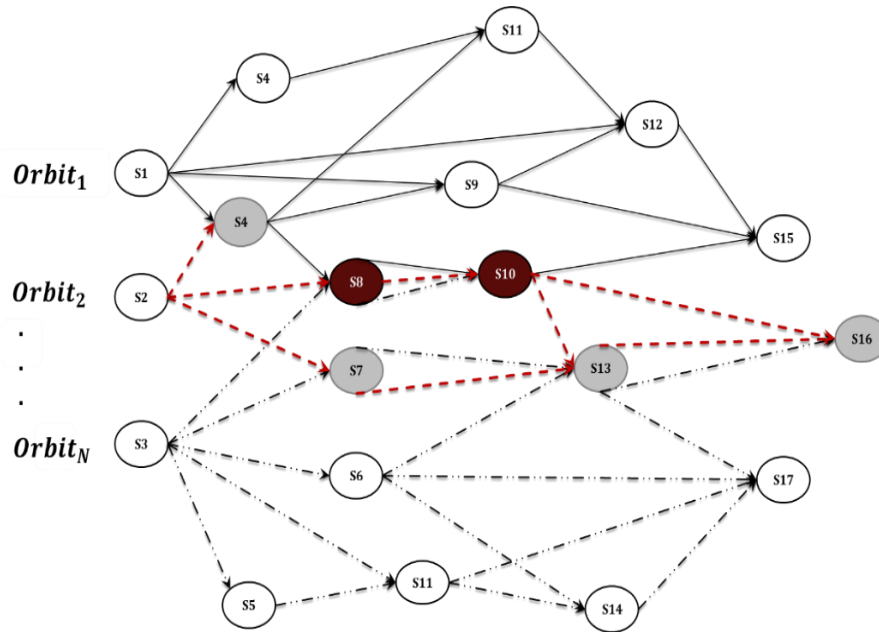


Figure No. 3: Acyclic directed graph model of a satellite constellation for observation scheduling

Finally, the input data for the SEOSR algorithm is containing a list of targets, each target has a list of possible strips obtained from several satellites. Maybe it appears conflict among strips of the same target. Besides, there are some information shall be appended with each strip, i.e., orbit number, the satellite ID, ts_{ki} , te_{ki} the start/end time of observation, a slewing angle θ_{ki} of strip S_k , and the *priority* (s_{ki}) within strip S_k .

3.5. SEOSR

A constructive heuristic probability for generating a path is the fundamental prime ingredient of an ACO algorithm. Therefore, N ants have put on randomly selected strips. Each Ant applies an arbitrary probability to decide which strip that visits later. Afterward, the feasible strip is appended to the path following the pheromone trail and heuristic information value. As shown

in lines 7-15 of Approach: SEOSR, when an ant k standing at the strip τ_i at iteration t , it will select the successor strip τ_j from its neighborhoods of unvisited strips \mathcal{N}_i^k into the same orbit with the following probability $\rho_{ij}^k(t)$:

$$\rho_{ij}^k(t) = \begin{cases} \frac{[\tau_{ij}(t)]^\alpha \cdot [\eta_{ij}]^\beta}{\sum_{l \in \mathcal{N}_i^k} [\tau_{il}(t)]^\alpha \cdot [\eta_{il}]^\beta} & \text{if } j \in \mathcal{N}_i^k \\ 0 & \text{otherwise} \end{cases} \quad (9)$$

Where τ_{ij} is a pheromone trail rallied in the edge from S_{ki} to S_{hl} . η_{ij} represents the heuristic information. α and β Represent the weights of pheromone and heuristic information. $J_k(i)$ represents the possible candidate successor strips of τ_i . Concerning the value of τ_o , it should be too low for preventing the system from going through further iterations. Furthermore, in order to exploit the heuristic information, some of the important features are considered to fulfill this issue. The η_{ij} is defined as follow:

$$\eta_{ij} = \frac{\omega_1 * p(s_{ki}) + \omega_2 * ty_{ki}}{\omega_3 * \theta_{ki} + \omega_4 * |\theta_{ki} - \theta_{lh}| + \omega_5 * ov_i} \quad (10)$$

Where $p(s_{ki})$ is a priority of a strip s_{ki} . The priority of the strip is considered by summing the priority of its points as shown in section 3.5.1. ty_{ki} is a type of strip s_{ki} , (i.e. emergency or normal target), the value is one when the strip belongs to an emergency target, otherwise zero. The primary principle behind this assumption is to increase the priority of an emergency strip in case of equality in the number of observations between the emergency strip and the normal one. θ_{ki} is a slewing angle for observing strip s_{ki} . $\theta_{ki} - \theta_{lh}$ is the time window for a transition to another position in the same swath width. And finally, ov_i is the number of conflicting points within the target t_i . The point is considered conflicted when it to be assigned to more than one strip for observation or observed before.

As shown in lines 14, 15 of Approach: SEOSR, after each selection, it should be verified the percentage of acceptance area ap_i of target t_i if it has been obtained. When the ratio of acceptance area ap_i of target t_i is satisfied, then, the target t_i associated with its different strips will be labelled as a target completed, and as a consequence, all its strips scheduled will be omitted from the plan. The more the slewing angle, and the time required to adjust the satellite its position for a new observation are large, and the more points that were previously observed in the candidate stripe, the less likely that this stripe will be scheduled. On the contrary, the emergency stripe, high priority, the higher the observation priority.

3.5.1. Priority calculation for a sector

After bringing through all possible strips, we need to mark them with the actual priority for observation first. On the other meaning, when a strip has several opportunities to be observed by several satellites at different times, the observation priority is come down. Our hypothesis is how to capture the strips that have few observation opportunities to be scheduled first. Often, these strips may be lost forever in case of a lack of observation early. To bring through less-popular-strips-rank (i.e., that strip has a few opportunities for observation), the Page Rank algorithm is developed in a novel form to construct the Strip-Rank algorithm. A strip does not consider instant when: 1) it is not come before by several important strips, which means the opportunity of observation come down as shown in Fig.3. On the other meaning, a strip does not consider instant as it has many important points that have a great opportunity for observation within several orbits with little slewing angles. 2) The number of voter strips (preceded strips) is not abundant. In contrast, the value of Strip-Rank comes down when the number of voter's strips has several other output-links, which means that the importance of them is divided by the number of their output-links. Therefore, this is a single factor that affects the score of the strip unfavorably. When the voters' strips are not important and few, the opportunity of observation of the strip is high. That means these strips may be lost if not observed early. On the other hand, the priority of a strip reaches the peak if the number of remained observation opportunities is just one.

To calculate the Strip-Rank of the strip $PR(s_k)$, a random walk was performed to eventually compute the score of all neighbours. The final score is divided by the number of output links. Recent studies were checked many damping factors (α) confirming that the suitable factor is 0.85 as mentioned by (El-Fishawy, N. et al 2014).

$$SR(s_{ki}) = \frac{1-\alpha}{N} + \alpha \sum_{s_{hl} \in N_{s_{ki}}} \left(\frac{SR(s_{hl})}{L(s_{hl})} \right) \quad (11)$$

Where N is the total number of strips. $N_{s_{ki}}$ is the list of candidates neighbours linked to the strip s_{ki} , $L(s_{hl})$ is the number of outbound links on strip s_{hl} . An initial strip rank is assigned for each strip equal to one. At each iteration, the Strip-Rank algorithm is called to update the ranking of strips according to Eq. 12.

$$p(s_{ki}) = 1/PR(s_{ki}) \quad (12)$$

After assigning each strip to a certain satellite, the Strip-Rank algorithm re-calculates the ranks of strips. This process continues until all strips are assigned to appropriate orbits.

3.5.2. Pheromone update rule

For trading off between exploitation and exploration in an optimization task, evaporate and update pheromone are two important processes to fulfill this issue. Consequently, when all ants found their solutions, the pheromone trails are initially evaporated within all edges to aid the ants to forget the precedent bad edges in later iterations. The pheromone trails reduced by a constant factor as follows:

$$\tau_{ij}(t) = (1 - \rho) \cdot \tau_{ij}(t) \quad (13)$$

Where ρ ($0 < \rho < 1$) is the pheromone evaporation coefficient. The following step is that each ant k deposits a pheromone quantity $\Delta\tau_{ij}(t)$ on the edges utilized according to how fineness of their solutions are. The main target of pheromone localized is the update mechanism to assist in reaching the global optimum solution.

$$\tau_{ij}(t) = [(1 - \rho) \cdot \tau_{ij}(t) + \sum_{k \in m} \Delta\tau_{ij}(t)^k]_{\tau_{min}}^{\tau_{max}} \quad (14)$$

Where $\Delta\tau_{ij}(t)$ is the amount of pheromone deposited by ant k on the edge (i, j) . Furthermore, adventitious updating by one solution on its edges to enhance the opportunity of selecting in the subsequent iterations. Expressly, the purpose of the pheromone updates phase is to reinforce the pheromone of better solutions in order to guide the search more intelligently.

$$\Delta\tau_{ij}(t) = \begin{cases} \frac{\sum_{j \in S^k(t)} \eta_{ij}}{Q} & \text{if } ij \in S^k(t) \\ 0 & \text{otherwise} \end{cases} \quad (15)$$

Where $S^k(t)$ is the best subset accumulated by ant k at iteration (t) , j represents the gathered stipes into the best path, and Q is the positive constant value. Besides, to prevent pheromone value from exploding and vacationing, the pheromone is restrained within a value range $[\tau_{max}, \tau_{min}]$, where τ_{max} and τ_{min} are the boundaries of the pheromone trail. This procedure is demonstrated in lines 19 of Approach: SEOSR

Approach: SEOSR

1. Divide the targets into a grid of points as shown in section 3.2;
2. Determine the intersection between the satellite's swath width and the targets as shown in section 3.3;
3. Obtain the probability of points as shown in section 3.5.1;
4. Construct the graph as shown in section 3.4;
5. Define pheromone and heuristic information, set parameters
 $Ant_s, \alpha, \beta, \omega_1, \omega_2, \omega_3, \omega_4, \omega_5, \tau_0, \tau_{max}, \tau_{min}, \rho, Max_i, Min_i$;
6. **While** $T < T_{max}$ **Do**
7. Randomly select number of Ant_n (strips) $\in S$, where $Ant_n == Ant_s$ and start to search a path in graph;
8. **For** each ant **Do**
9. Construct a candidate list $\mathcal{N}_i^k(i)$ according to Eq. 10;
Obtain the probability of strips within the candidate list $\mathcal{N}_i^k(i)$;
10. **If** $\mathcal{N}_i^k(i) \neq \emptyset$
11. Select a strip s_i in a $\mathcal{N}_i^k(i)$ that has the highest priority;
12. Add the selected strip to the partial solution;
13. Remove the strip s_{ki} from candidate list $\mathcal{N}_i^k(i)$;
14. **If** the acceptance area ap_i of target t_i has been obtained;
15. Remove a target t_i associated with its strips s_{ki} from constructed graph;
16. Record the solutions generated by the colony in this generation;
17. **If** $S^N \geq S^0$
18. $S^0 = S^N$;
19. Evaporate, and update pheromone on the visited edges according to Eq. 13, 14, and 15;
20. **If** $NC \geq Min_i$
21. **If** $NC = Max_i$
22. $NC = NC + 1$;
- 23.
24. **End**

4. Computational results & analysis

In this section, the parameter setting for the SEOSR algorithm is discussed and computational results are presented.

4.1 Simulated instances

Since there are yet not benchmark test problems in the satellite scheduling research subject area, a random generation mechanism is produced to test algorithms. The test problems are generated according to the following rules: 1) targets generated within an area range between north latitude $20^\circ \sim 50^\circ$ and east longitude $70^\circ \sim 130^\circ$. Eight practical simulated instances tested

are used in this research. Each satellite circles the earth within 100 minutes each time and runs about 14 orbits a day. Sensors on satellites can slew horizontally among angle range $[-33, 33]$. Each group includes several targets, each divided into many strips, each divide into a set of points. The targets are randomly distributed on the earth's surface with latitude among $[-33, 60]$ and longitude among $[0, 153]$. Time-windows and slewing angles associated with targets and their satellites have been calculated before use Analytical Graphics Inc.'s professional software named Satellite Tool Kit, also known as the STK. The basic information of eight practical instances is given in Table 1

Table No. 1: The constitutional information of the practical simulated instances

Instance #	Num. of satellite	Num. of antennas	Num. of targets	Num. of Strips	Num. of edges	Scheduling period
S01	7	5	20	420	2993	2018/05/4–24
S02	10	7	25	480	3337	2018/05/4–25
S03	12	9	30	465	3250	2018/06/8–28
S04	15	10	40	501	3988	2018/06/10–24
S05	17	11	45	522	4200	2018/07/10–27
S06	18	12	50	593	4338	2018/07/12–28
S07	19	13	55	634	5009	2018/07/19–29
S08	20	15	60	688	5055	2018/08/18–28

Firstly, the influence of changing the parameters has been empirically studied using various settings of thirty independent executions of the algorithms based on instance #8. Moreover, the maximum iteration number is 150. **Ant_Size**, evaporation rate ρ , initial pheromone trail τ_0 , the different kinds of heuristic weights ($\omega_1, \omega_2, \omega_3, \omega_4, \omega_5$), pheromone, and heuristic information weights (α, β) are varied among candidate values except one parameter keeps unchanged. The default value of each parameter is $\alpha = 1$, $\beta = 2$, $r = 5$, **Ant_Size** = 15, $\tau_0 = 0.4$, $\rho = 0.01$. The parameter ranges are listed in table 2.

Table No. 2: Parameters ranges of SEOSR

Parameter	Range
Ant_Size	{5, 8, 10, 12, 15, 20}
ρ	{0.01, 0.03, 0.05, 0.07, 0.09, 0.1}
τ_0	{0.001, 0.005, 0.01, 0.015, 0.02, 0.03}
$\omega_1, \omega_2, \omega_3, \omega_4, \omega_5$	{(0.1, 0.2, 0.2, 0.3, 0.2), (0.2, 0.2, 0.1, 0.3, 0.2), (0.2, 0.3, 0.2, 0.1, 0.2), (0.1, 0.2, 0.2, 0.2, 0.3), (0.2, 0.2, 0.1, 0.2, 0.3), (0.3, 0.2, 0.2, 0.1, 0.2)}
α, β	{(0.5, 1), (1, 0.5), (0.5, 1.5), (1.5, 0.5), (0.5, 2), (2, 0.5)}

The final experimental results are represented in the form of box plots as shown in figure. 4. The algorithm execution is vacillating with the ants' size. With a small value of ants' size, solution fineness is often declined. Whereas **Ant_Size** exacerbates, further candidate solutions can be generated at each cycle, but the goodness of solutions hasn't been enhanced. The optimal solution obtained from each iteration is often dominant. This may be due to the collaboration among ants. Consequently, when the number of ants equals ten, the trade-off between the maximum and the minimum number of ants is adapted to overcome this gap.

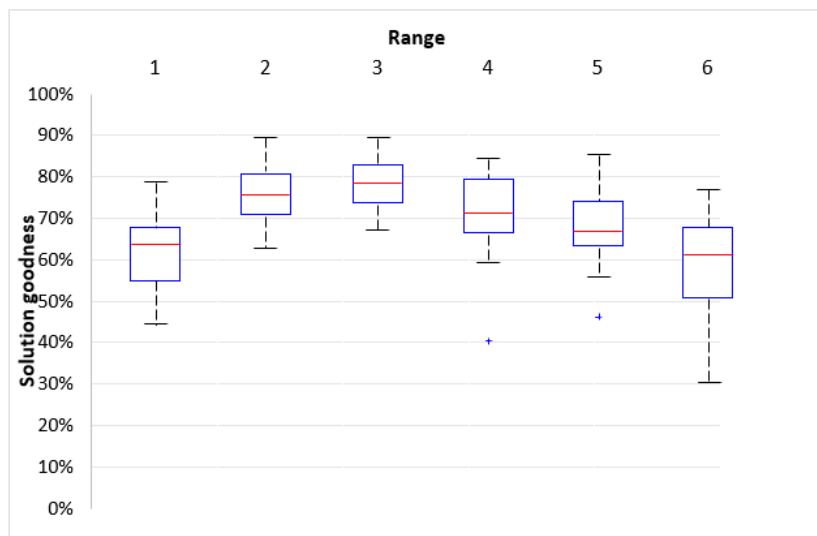


Figure No. 4: Box-plot for the algorithm performance with various ant number **Ant_Size**

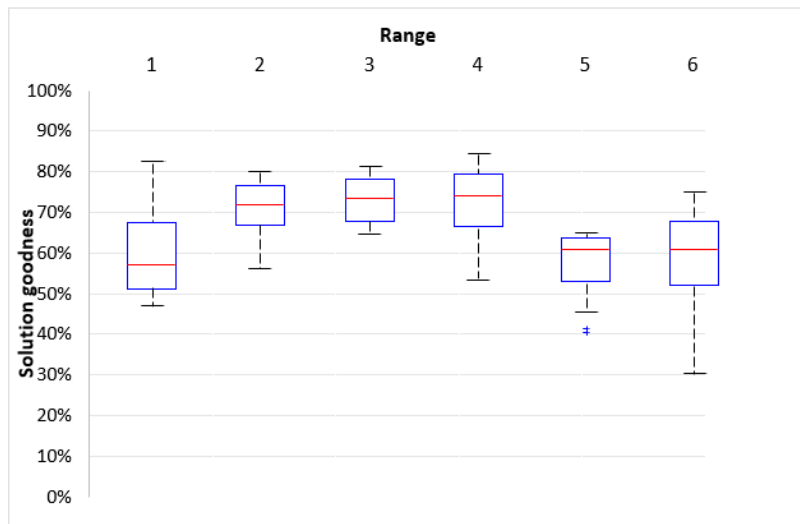


Figure No. 5: Box-plot for the algorithm performance with various evaporation rate ρ

Figure. 5 shows the algorithm's fulfillment varying with ρ . It can be observed that the finance solution declines and the gap between maximum and minimum increases with growing the value of ρ . In particular, the performance of the algorithm is bad greatly as ρ is equal to 0.1.

This is due to the higher ρ , the skewness appears in the pheromone trails. As a result, the search converges earlier around the best run.

Figure. 6 shows the solution performance varying with τ_0 . The performance of the algorithm is the worst when τ_0 is equal to 0.001 and 0.005. The corresponding solution results are not very satisfying when the value of τ_0 is too little or too high.

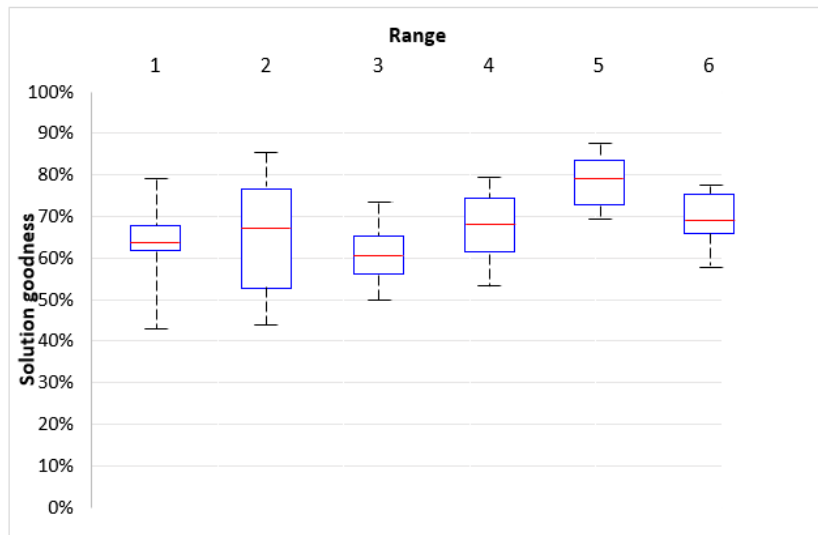


Figure No. 6: Box-plot for the algorithm performance with various initial pheromone trail τ_0

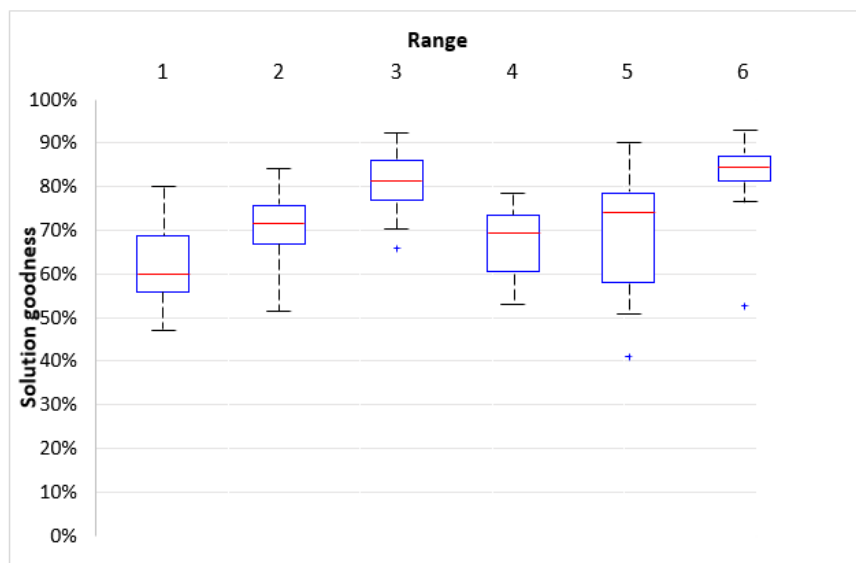


Figure No. 7: Boxplot for the algorithm performance with various kinds of heuristic information $\omega_1, \omega_2, \omega_3, \omega_4, \omega_5$

Figure. 7 shows the algorithm performance varying with ($\omega_1, \omega_2, \omega_3, \omega_4, \omega_5$) that symbolize the weights of heuristic information types. It has been noticed that the optimal solution quality

is captured when the values of $\omega_1, \omega_2, \omega_3, \omega_4, \omega_5$ parameters are 0.3, 0.2, 0.2, 0.1, 0.2 respectively.

Figure. 8 shows the algorithm performance varying in α and β parameters that represent the weights of pheromone amount and heuristic information. It is observed that there is no remarkable variation when the amount of the α parameter is assigned from zero to one. In contrast, when the β parameter is assigned a value higher than 1, stagnation appears. The best values are obtained when α, β parameters are 1.5, and 0.5 respectively.

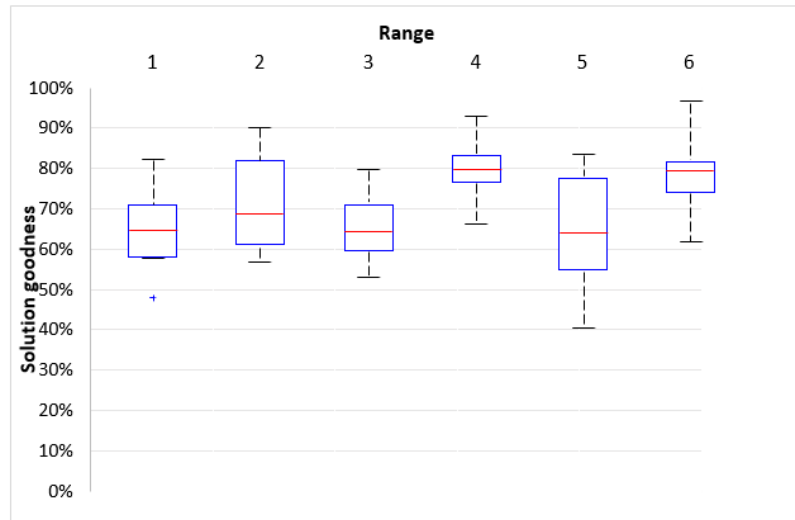


Figure No. 8: Boxplot for the algorithm performance with various weights of pheromone and heuristic information α, β

Ultimately, after thirty independent executions of each scenario, the maximal performance obtained as the parameters' values as shown in Table NO. 3. according to our empirical experiments.

Table No. 3: optimal parameters value of SEOSR

Parameter	Value	Parameter	Value
<i>Ant_Size</i>	10	ω_5	0.2
α	1.5	τ_0	0.02
β	0.5	τ_{max}	1
ω_1	0.3	τ_{min}	0.001
ω_2	0.2	ρ	0.05
ω_3	0.2	<i>Max_iteration</i>	100
ω_4	0.1	<i>Min_iteration</i>	30

4.1. Computational results

To assess the effectiveness of the SEOSR approach, we also compared it with a mixed-integer linear program (MILP) (Augenstein, S. et al. 2016), NSGA-II (Shao, X. et al. 2016), ACO-LS

algorithm (Zhang, Z. et al. 2014), simulated annealing algorithm (SA) (Wu, G. et al. 2017). Some algorithms used task grouping because it was possible to collect more than one point at the same time. In our case, the targets are strips (i.e., a collection of points), therefore there is no need for the clustering concept. Additionally, the width of the camera equals the width of the strip. A mixed-integer linear program (MILP) approach boosts for generating schedules for all satellites and ground stations in a network (Augenstein, S. et al. 2016). A non-dominated sorting genetic algorithm-II-based (NSGA-II) multi-objective optimization (MOO) method was developed to solve the MOO planning task of satellite flying formation systems. Two principal objectives are considered to maximize total profits and completed acquisition figures (Shao, X. et al. 2016). ACO-LS algorithm of multi-satellite control resource scheduling (Zhang, Z. et al. 2014) is developed depending on ant colony optimization. The main algorithm relies on updating the pheromone pathway with two stages to avoid getting trapped in the cycling ants. Targeting to minimize the visible arc as a fitness function. Where the visible arc contains eight elements (satellite No., orbit data/time, service equipment, highest elevation angle, start/end time of observation, and satellite direction). The optimization objective is to minimize the working extent for satisfying all the demanded tasks. Finally, authors (Wu, G. et al. 2017) demonstrate a great strategy to improve the effectiveness of the satellite schedule. Adaptive simulated annealing-based scheduling task incorporation with a dynamic task clustering strategy (ASA-DTC) developed for satellite observation scheduling problems. The parameters of algorithms are set by (Augenstein, S. et al 2016), (Shao, X. et al 2016), (Zhang, Z. et al 2014), and (Wu, G. et al 2017).

All of the comparison algorithms have been re-implemented and experimented with the same data. Thirty independent executions of the algorithms for each scenario are conducted, ultimately the average result is accounted for. The effectiveness of the SEOSR approach and other approaches examined. The results are plotted in Figures 9 and 10. Where Figure 9. shows the number of strips that have been observed through each algorithm, while Figure No. 10 shows the number of targets that have been observed. The two figures show the SEOSR approach outperforms all other algorithms in all scenarios. Thus, we can safely come to two conclusions: (1) SEOSR is a competitive algorithm to solve multi-satellite resources scheduling tasks; (2) The PageRank technique noticeably improves the performance of scheduling tasks. Eventually, from Figure 11 we see the average effectiveness of the different algorithms. Where we notice that the proposed algorithm has reached more than 90% efficiency compared to other methods.

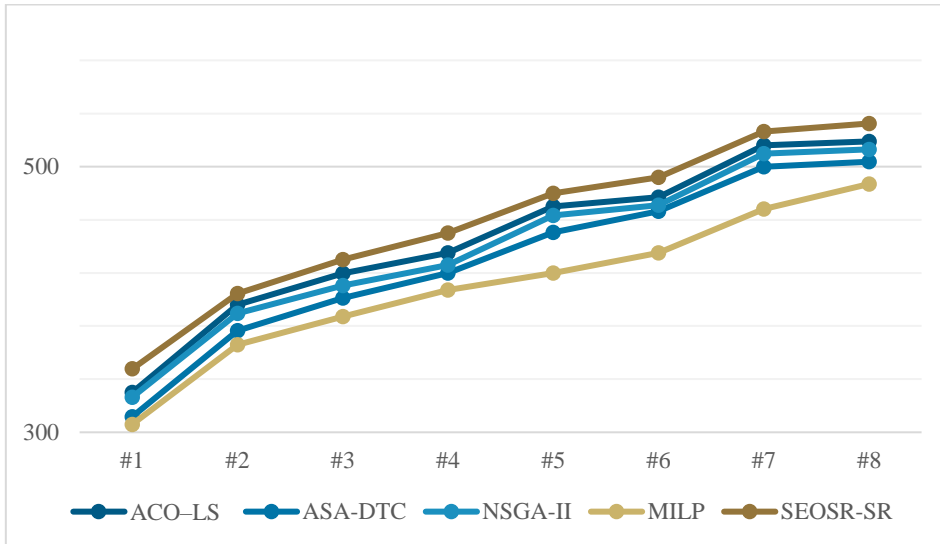


Figure No. 9: Effectiveness of different algorithms in terms of number of strips.

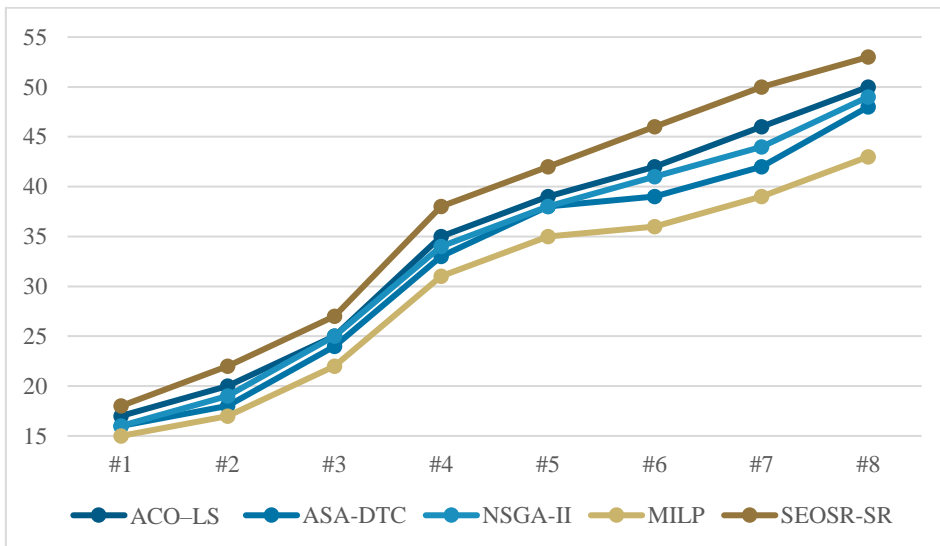


Figure No. 10: Effectiveness of different algorithms in terms of number of targets.

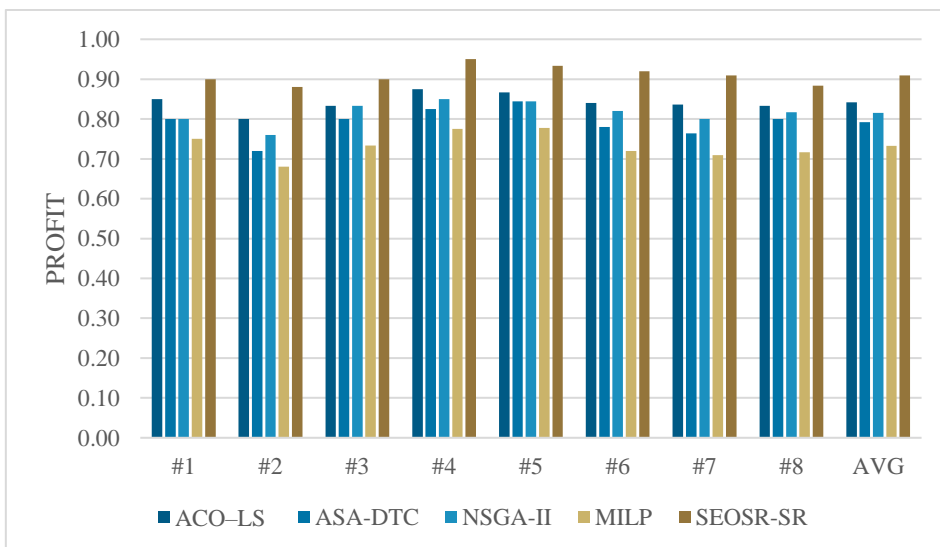


Figure No. 11: Average effectiveness of different algorithms.

On the other hand, figures 12 and 13 show the performance of gross profit in terms of priority in response to fewer observation opportunities. We performed experiments to compare the scheduling results obtained by SEOSR with and without the consideration of priority (shortly denoted by SR and Non-SR, respectively). The comparison is displayed in figure 12 and figure 13 from which we discover that calculating the priority of target significantly improves the fineness of the solution of each scenario especially when the problem size becomes larger. In general, observation based on priority has several advantages. First, increases the overall profit of the targets. Second, reduces the conflict between strips observed. Third, prevents the targets from being lost by observing the required percentage of them to be accepted. Finally, keep the satellite's resources from misuse.

Also, an experiment in the term of computation times is conducted to compare the running times of the proposed SEOSR against other algorithms for eight instances. As it is clear from figure 14, by growing the number of requested tasks in the problems, the running times of all algorithms are increased. Besides, the proposed SEOSR algorithm and the ACO-LS algorithm have a high uptime compared to the other algorithms in all cases. The complexity is known because the ACO algorithm is higher than other algorithms. While it is the most efficient and consistent in solving such complex problems. Therefore, we may notice that one of the most prominent drawbacks that ACO-based algorithms may face is the runtime.



Figure No. 12: Performance influences of task priority in terms of number of strips.

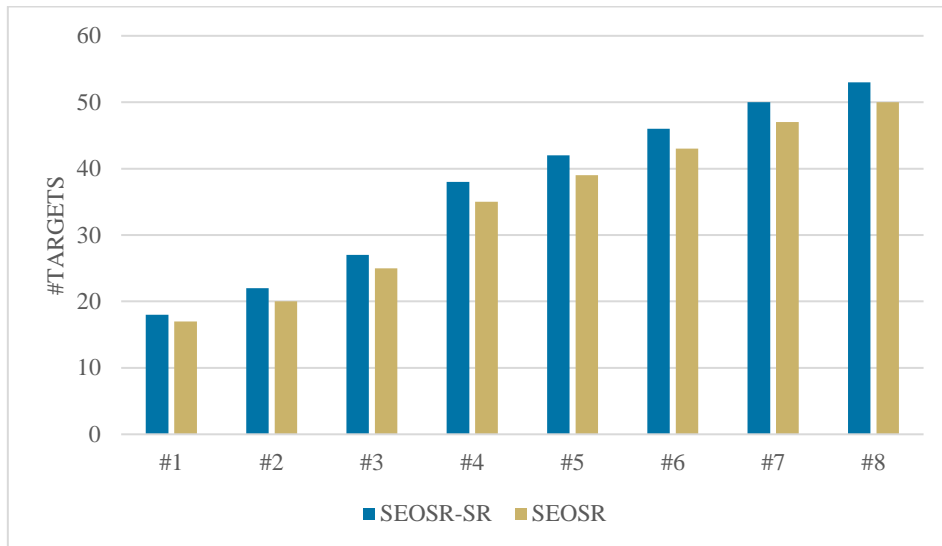


Figure No. 13: Performance influences of task priority in terms of number of targets.

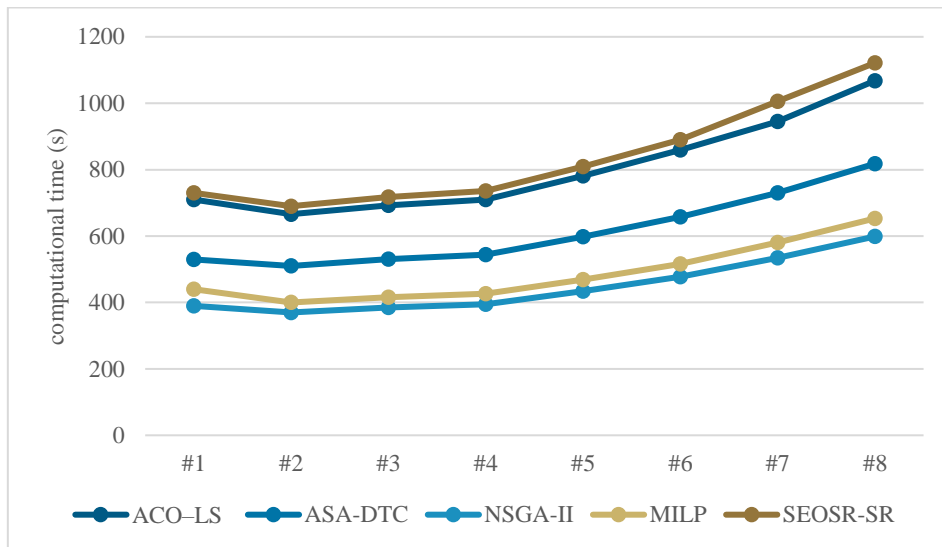


Figure No. 14: Efficiency of different algorithms.

5. Conclusion and future work

In this work, considering the priority of tasks into the scheduling in a novel shape can improve the effectiveness of satellite observation systems. Since both calculating strip priority and scheduling process are integrated. Firstly, each target is transferred into a list of points, subsequently, many (conflicted) strips. The priority of all points is accounted for according to the number of likely observations. A brilliant PageRank algorithm is employed to calculate the actual priority of each point. Next, an acyclic directed model and the ACO algorithm were developed to obtain high-quality schedules. To enhance the scheduling task and achieve the percentage of acceptance for all targets, we considered the priority algorithms to prevent the target to be omitted. Extensive experimental simulations demonstrate that the SEOSR

algorithm is capable of finding optimal or near-optimal solutions at a reasonable computational cost. Our comparison tests show that SEOSR outperforms some other algorithms like SA and MILP.

The future work in our study aims to transform the scheduling task into a multi-objective optimization task using new optimization algorithms. Design dynamic scheduling mechanisms to enable a quick response to unexpected situations, such as cloud disturbances.

6. References

- [1] Baek, S.-W., Han, S.-M., Cho, K.-R., Lee, D.-W., Yang, J.-S., Bainum, P. M., et al. (2011). Development of a scheduling algorithm and GUI for autonomous satellite missions. *Acta Astronautica*, 68, 1396–1402.
- [2] Barbulescu, L., Howe, A. E, Watson, J.-P., & Whitley, L. D (2002). Satellite range scheduling: A comparison of genetic, heuristic and local search. In *Parallel problem solving from nature—PPSN VII* (pp. 611–620). Springer.
- [3] Bianchessi, N., Cordeau, J.-F., Desrosiers, J., Laporte, G., & Raymond, V. (2007). A heuristic for the multi-satellite, multi-orbit and multi-user management of earth observation satellites. *European Journal of Operational Research*, 177, 750–762.
- [4] Chen, Y., Zhang, D., Zhou, M., & Zou, H. (2012). Multi-satellite observation scheduling algorithm based on hybrid genetic particle swarm optimization. In *Advances in Information Technology and Industry Applications* (pp. 441–448). Springer.
- [5] El-Fishawy, N., Hamouda, A., Attiya, G. M., & Atef, M. (2014). Arabic summarization in twitter social network. *Ain Shams Engineering Journal*, 5(2), 411-420.
- [6] Frank, J., Jonsson, A., Morris, R., & Smith, D. (2001). Planning and scheduling for fleets of earth observing satellites. In *Proceedings of the sixth international symposium on artificial intelligence, robotics, automation and space*.
- [7] Gao, K., Wu, G., & Zhu, J. (2013). Multi-satellite observation scheduling based on a hybrid ant colony optimization. *Advanced Materials Research*, 765–767, 532–536.
- [8] Marinelli, F., Nocella, S., Rossi, F., & Smriglio, S. (2011). A Lagrangian heuristic for satellite range scheduling with resource constraints. *Computers & Operations Research*, 38, 1572–1583.
- [9] Mosa, M. A. (2019a). Real-time data text mining based on Gravitational Search Algorithm. *Expert Systems with Applications*, 137, 117-129.
- [10] Mosa, M. A. (2020). Data Text Mining Based on Swarm Intelligence Techniques: Review of Text Summarization Systems. In *Trends and Applications of Text Summarization Techniques* (pp. 88-124). IGI Global.
- [11] Mosa, M. A., Anwar, A. S., & Hamouda, A. (2019b). A survey of multiple types of text summarization with their satellite contents based on swarm intelligence optimization algorithms. *Knowledge-Based Systems*, 163, 518-532. DOI.org/10.1016/j.knosys.2018.09.008.
- [12] Mosa, M. A., Hamouda, A., & Marei, M. (2017a). Ant colony heuristic for user-contributed comments summarization. *Knowledge-Based Systems*, 118, 105-114.
- [13] Mosa, M. A., Hamouda, A., & Marei, M. (2017b). Graph coloring and ACO based summarization for social networks. *Expert Systems with Applications*, 74, 115-126.
- [14] Mosa, M. A., Hamouda, A., & Marei, M. (2017c). *How can Ants Extract the Essence Contents Satellite of Social Networks?* LAP Lambert Academic Publishing, ISBN: 978-3-330-32645-3.

- [15] Pandey, V., Malhotra, A., Kant, R., & Sahana, S. K. (2019, July). Solving Scheduling Problems in PCB Assembly and Its Optimization Using ACO. In *International Conference on Swarm Intelligence* (pp. 243-253). Springer, Cham.
- [16] Sarkheyli, A., Vaghei, B. G., & Bagheri, A. (2010). New tabu search heuristic in scheduling earth observation satellites. In *2010 2nd International conference on software technology and engineering (ICSTE)* (Vol. 2, pp. V2-199–V192-203): IEEE.
- [17] Thiruvady, D., Blum, C., & Ernst, A. T. (2019, January). Maximising the Net Present Value of Project Schedules Using CMSA and Parallel ACO. In *International Workshop on Hybrid Metaheuristics* (pp. 16-30). Springer, Cham.
- [18] Zhang, N., Feng, Z., & Ke, L. (2011). Guidance-solution based ant colony optimization for satellite control resource scheduling problem. *Applied Intelligence*, 35, 436–444.
- [19] Zhu, K., Li, J., & Baoyin, H. (2010). Satellite scheduling considering maximum observation coverage time and minimum orbital transfer fuel cost. *Acta Astronautica*, 66, 220–229.
- [20] Zufferey, N., Amstutz, P., & Giaccari, P. (2008). Graph colouring approaches for a satellite range scheduling problem. *Journal of Scheduling*, 11, 263–277.
- [21] Zhang, Z., Zhang, N., & Feng, Z. (2014). Multi-satellite control resource scheduling based on ant colony optimization. *Expert Systems with Applications*, 41(6), 2816-2823.
- [22] Lee, J., Kim, H., Chung, H., Kim, H., Choi, S., Jung, O., & Ko, K. (2018). Schedule Optimization of Imaging Missions for Multiple Satellites and Ground Stations Using Genetic Algorithm. *International*
- [23] Sarkheyli, A., Bagheri, A., Ghorbani-Vaghei, B., & Askari-Moghadam, R. (2013). Using an effective tabu search in interactive resources scheduling problem for LEO satellites missions. *Aerospace Science and Technology*, 29(1), 287-295.
- [24] Augenstein, S., Estanislao, A., Guere, E., & Blaes, S. (2016, March). Optimal scheduling of a constellation of earth-imaging satellites, for maximal data throughput and efficient human management. In *Twenty-Sixth International Conference on Automated Planning and Scheduling*.
- [25] Shao, X., Zhang, Z., Wang, J., & Zhang, D. (2016). NSGA-II-Based Multi-objective Mission Planning Method for Satellite Formation System. *Journal of Aerospace Technology and Management*, 8(4), 451-458.
- [26] Wu, G., Wang, H., Pedrycz, W., Li, H., & Wang, L. (2017). Satellite observation scheduling with a novel adaptive simulated annealing algorithm and a dynamic task clustering strategy. *Computers & Industrial Engineering*, 113, 576-588.